Optical and Quantum Electronics **33:** 373–386, 2001.

Modal analysis of rib waveguide through finite element and mode matching methods

STEFANO SELLERI[1] AND JIŘÍ PETRÁČEK[2]*
[1] *Dipartimento di Ingegneria dell'Informazione, University of Parma, Parco Area delle Scienze 181A, 43100 Parma, Italy (E-mail: selleri@kao.tlc.unipr.it)*
[2] *Institute of Physical Engineering, Brno University of Technology, Technická 2, 616 69 Brno, Czech Republic*
*(*author for correspondence: E-mail: j.petracek@fyzika.fme.vutbr.cz)*

Abstract. Two mode solvers based on the finite element and the mode matching methods are compared by way of analyzing rib waveguides. Differences between the normalized propagation constants provided by the two methods are always less than 10^{-4} which is at least about one order of magnitude smaller than previously reported values. Results for lossy waveguides and field comparison are also presented.

Key words: dielectric waveguides, finite element method, integrated optics, mode matching method

1. Introduction

Modal analysis is an important issue in the simulation of photonic devices as the knowledge of the propagation constant and the field distribution of the propagating modes allows a deep investigation of the characteristics and the performances of a given device. Many numerical methods have been proposed to deal with problems where an analytical solution is not available. Amongst them there are number of rigorous methods, like the finite difference method (FDM), the finite element method (FEM), the spectral-domain method, the method of lines and the mode matching method (MMM). These methods have been studied for many years and achieved wide acceptance for their efficiency and reliability. In spite of this, it is quite difficult to find, in the scientific literature, exhaustive and complete comparisons of their performances. In particular, many published comparisons often lack in checking the field distribution accuracy while focusing on the values of the propagation constant. Moreover the effects of gain and/or loss are neglected thus restricting the analysis to the simple real case.

It was suggested in the last review (Vassallo 1997) that a rigorous method should provide exact three-digit values for normalized propagation constant B. It also means that differences ΔB amongst B calculated with various such methods should be less than 0.001. Comparison of results obtained with

MMM and the other already mentioned methods showed that this criterion is not always fulfilled. The worst results were obtained for FEM and FDM with $|\Delta B| > 0.003$ in some cases. This led to the conclusion that, assuming the mode matching, also called modal transverse resonance method, as the reference, the other methods can also provide 'an exact third digit in B'; however FEM and FDM cannot do it so easily (Vassallo 1997). For what concerns the FEM, this conclusion has been drawn on the basis of a comparison with data read from a curve presented by Rahman and Davies (1985) and with values provided by Koshiba *et al.* (1994) using formulations based on simple constant or linear edge elements.

This paper will concentrate on comparison of FEM and MMM only, with the attempt to update the results reported in (Vassallo 1997) through a true and active interaction between two research groups involved for several years in the development of the FEM and the MMM, respectively at the Department of Information Engineering of Parma University, Italy, and at the Institute of Physical Engineering, Brno University of Technology, Czech Republic. The aim is to show that much better agreement than that reported in (Vassallo 1997) can be achieved between the two methods. In particular the attention is focused on rib waveguides, which have been studied, in the past, for different values of the wavelength, layer width and refractive indices, being thus widely assumed as a benchmark for both modal (Vassallo 1997) and propagation (Vincetti *et al.* 2000) analysis.

Besides the cited papers and references therein, recent analysis of rib waveguides have been reported in Ramm *et al.* (1997), Yamauchi *et al.* (1998), Koshiba and Tsuji (2000) and Tsuji and Koshiba (2000). In Ramm *et al.* (1997) a multigrid eigenvalue solver based on the FDM has provided very accurate results for the quasi-TE case. A comparison between MMM and a FDM beam propagation formulation is given in Yamauchi *et al.* (1998) showing a three digit, or even a four-digit agreement in B. Further analysis based on FEM approaches mainly focused on the description of adaptive mesh generation algorithms (Tsuji and Koshiba 2000) or on the implementation of high order and curvilinear hybrid edge-nodal elements (Koshiba and Tsuji 2000).

The cross-section of such rib waveguide and the definition of the parameters used in the paper are shown in Fig. 1. Values provided by the MMM and the FEM for the normalized propagation constant B, defined as

$$B = \frac{n_{\text{eff}}^2 - n_{\text{s}}^2}{n_{\text{c}}^2 - n_{\text{s}}^2}$$

n_{eff}, n_{s} and n_{c} being the numerically evaluated effective mode index, the substrate refractive index and the core one respectively, agree up to and including the fourth digit after the decimal point.

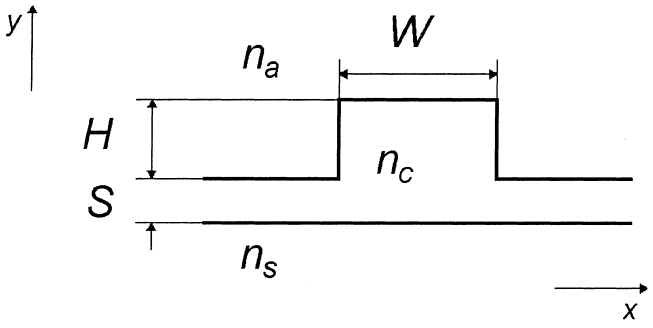

Fig. 1. Rib waveguide notation. n_a, n_c and n_s are refractive indices of superstrate, core and substrate; S, H and W define the waveguide geometry.

In addition, a comparison of vector field distributions of the rib modes is presented, for the first time, in order to investigate accuracy on the evaluated field components rather than just on propagation constant. Finally, the paper presents results for lossy waveguides very rarely assumed as benchmark for comparison of different numerical methods.

The paper is organized as follows. In Section 2, the used FEM and MMM are briefly presented in order to clearly describe the formulations, the working conditions and the techniques assumed for the problem resolution. In Section 3 the results concerning the analysis of different rib structures, at different wavelengths, and with real and complex refractive indices are discussed. Conclusions are given in Section 4.

2. Finite element and mode matching methods

Both methods used for the comparison are full vector and can analyze waveguides with complex profile of refractive index.

2.1. FINITE ELEMENT METHOD

The FEM allows the cross-section of the waveguide in the transverse x-$y$plane to be divided into a patchwork of triangular elements which can be of different sizes, shapes, refractive indices and anisotropies. In this way any kind of geometry, including circular, elliptic or oblique interfaces, as well as medium characteristic can be accurately described.

The considered formulation is based on the curl–curl equation. For a medium described by the relative dielectric permittivity ε_r and the magnetic permeability μ_r it reads:

$$\overline{\nabla} \times \left(p\overline{\nabla} \times \bar{V}\right) - k_0^2 q \bar{V} = 0 \tag{1}$$

where p and q represent ε_r^{-1} and μ_r when $\bar{V}$ is the magnetic field $\bar{H}$ and μ_r^{-1} and ε_r when $\bar{V}$ is the electric field $\bar{E}$; $k_0 = (\mu_0 \varepsilon_0)^{1/2}$ is the wave number in the vacuum. By applying the variational finite element procedure, the full vector equation (1) yields the algebraic problem (Selleri *et al.* this issue):

$$([A] - (n_{\text{eff}})^2[B])\{u\} = 0 \tag{2}$$

where $\{u\}$ is the unknown eigenvector representing the magnetic or the electric field while the eigenvalue directly provides the complex effective mode index n_{eff}. The matrices $[A]$ and $[B]$ are sparse and symmetric thus allowing an efficient resolution of Equation (2) by means of high performance algebraic solvers for both real and complex problems (Arpack Software).

High order T_{15} edge elements, according to Webb definition (Dillon *et al.* 1994), are considered. They employ six Lagrangian basis functions for the longitudinal component while, for the transverse one, six tangential plus two inner normal unknowns, rather than just constant or linear edge elements as in Koshiba *et al.* (1994) and Tsuji and Koshiba (2000). Edge elements avoid spurious modes that pollute the guided mode spectrum. Neumann and Dirichlet boundary conditions have been assumed on the outer boundary which has been moved far away from the rib region in order not to affect the numerical solution. To this aim, the position of the outer border is retained when stable solutions are computed, whatever the imposed boundary conditions. Meshes constructed following this criterion present an high number of elements, actually useless, which could be reduced by using more efficient boundary conditions as the radiation ones (Hernandez-Figueroa *et al.* 1995) or those based on anisotropic layers (Cucinotta 2000).

It is important to point out that the accuracy of the proposed approach has already been checked in Selleri and Zoboli (1997) through comparisons with the analytical solutions of step fibers and metallic waveguides.

2.2. MODE MATCHING METHOD

The cross-section of a waveguide similar to that in Fig. 1 is divided into a sequence of sections, which are separated by vertical lines. Each section can be viewed as a part of a 2D waveguide (the refractive index in each section is a function of y coordinate only) and TE and TM modes of such a 2D waveguide can be found and normalized. The mode matching method (Oliner *et al.* 1981; Peng and Oliner 1981; Sudbø 1993) is based on the expansion of the unknown modal field into these TE and TM mode pairs in each section. Consequently tangential components of the modal field are matched at the section interfaces and this results in a nonlinear eigenvalue problem for

the effective mode index. The spatial resolution of the method depends on the number of TE/TM mode pairs used (Vassallo 1997).

The spectrum of radiation modes for each 2D waveguide has to be discretised and this is achieved by closing computational domain in y direction by electric or magnetic conductors. Note, however, that the computational domain is not limited in x direction, except possible walls resulting from waveguide symmetry.

Here the matrix formulation of MMM (Sudbø 1993) is used. The eigenvalue problem has the form

$$[M(n_{\text{eff}})]\{u\} = 0$$

where $\{u\}$ is the eigenvector corresponding with amplitudes of TE/TM mode pairs, the matrix $[M]$ has a band structure and its elements are nonlinear functions of n_{eff}. The problem was solved by searching for roots of determinant of $[M]$ with the inverse iteration technique. The 'root tracking' technique was used to find eigenvalues in the complex plane.

In order to analyze structures with loss, the TE and TM modes of the 2D waveguides are normalized using the general orthogonality relations derived in Bresler *et al.* (1958) and these relations are also employed in the matching procedure.

3. Results and discussion

In this section magnetic field based FEM and MMM formulation results for various rib structures are compared. The computational window included only symmetric half of the rib waveguide, and electric or magnetic perfect conductors were assumed along the vertical symmetry line to look for quasi-TE and quasi-TM solutions respectively. The results from the both methods were stabilized with respect to the spatial resolution and the size of the computational domain. It also means that the results do not depend on the type of artificial boundaries (electric or magnetic conductors) which close computational domain except vertical symmetry line. These points were checked by means of repeated calculations with different number of TE/TM mode pairs or with different number of mesh elements for MMM and FEM respectively, and by means of repeated calculations with the both kinds of artificial boundaries.

The first example is a rib waveguide with the parameters: $W = 2\,\mu\text{m}$, $H = 1.1\,\mu\text{m}$, $S = 0.2\,\mu\text{m}$, $n_{\text{a}} = 1$, $n_{\text{c}} = 3.44$ and $n_{\text{s}} = 3.34$, working in the third telecommunication window at $\lambda = 1.55\,\mu\text{m}$. This waveguide has been widely considered as basic structure for integrated optics devices and has been studied by several research groups, as can be noted in Ramm *et al.*

Table 1. Convergence of B for dominant modes calculated with MMM[a]

L	Δy (μm)	B, quasi-TE	B, quasi-TM
25	0.19	0.483965	0.476253
50	0.095	0.483409	0.475102
100	0.048	0.483341	0.474996
200	0.024	0.483325	0.474991
300	0.016	0.483323	0.474991
600	0.0080	0.483321	0.474992
1000	0.0048	0.483321	0.474992

[a] L is the number of TE/TM mode pairs used and Δy is corresponding spatial resolution. The rib waveguide parameters are $W = 2\,\mu\text{m}$, $H = 1.1\,\mu\text{m}$, $S = 0.2\,\mu\text{m}$, $n_a = 1$, $n_c = 3.44$, $n_s = 3.34$ and $\lambda = 1.55\,\mu\text{m}$.

(1997), Koshiba and Tsuji (2000), Tsuji and Koshiba (2000) and Vincetti *et al.* (2000) and references therein. Table 1 shows convergence of B calculated with the MMM for dominant modes. The figures for quasi-TE mode were obtained with magnetic conductors placed 0.5 μm above the rib and 3 μm below the guiding layer while electric conductors at the same positions were used in quasi-TM case. Results of FEM calculation are shown in Table 2, the dimensions of the computational windows used are as in Figs. 2 or 3 and all artificial boundaries are electric conductors. According Tables 1 and 2, the stable MMM results are $B = 0.48332$ for quasi-TE mode and $B = 0.47499$ for quasi-TM mode while the stable FEM results are $B = 0.48331$ for quasi-TE mode and $B = 0.47497$ for quasi-TM mode. These five digit values do not depend on artificial boundaries used. The two methods provide results in excellent agreement and the differences of the B values suggest that four-digit accuracy is achieved.

Note that data reported in the literature for this rib waveguide often differ on the fourth or fifth digit in the computed effective mode index while this accuracy has here been obtained for the normalized propagation constant.

The obtained value for the quasi-TE mode is supported also by the result $B = 0.48331$ provided in Ramm *et al.* (1997) through a finite difference

Table 2. Convergence of B for dominant modes calculated with FEM. N is number of elements used[a]

quasi-TE		quasi-TM	
N	B	N	B
575	0.483253	581	0.474894
771	0.483276	761	0.474929
1190	0.483290	1180	0.474958
1440	0.483297	1425	0.474964
1902	0.483300	1930	0.474964
2333	0.483305	2391	0.474970
2556	0.483305	2586	0.474972
2795	0.483305	2843	0.474972

[a] The waveguide is the same as in Table 1.

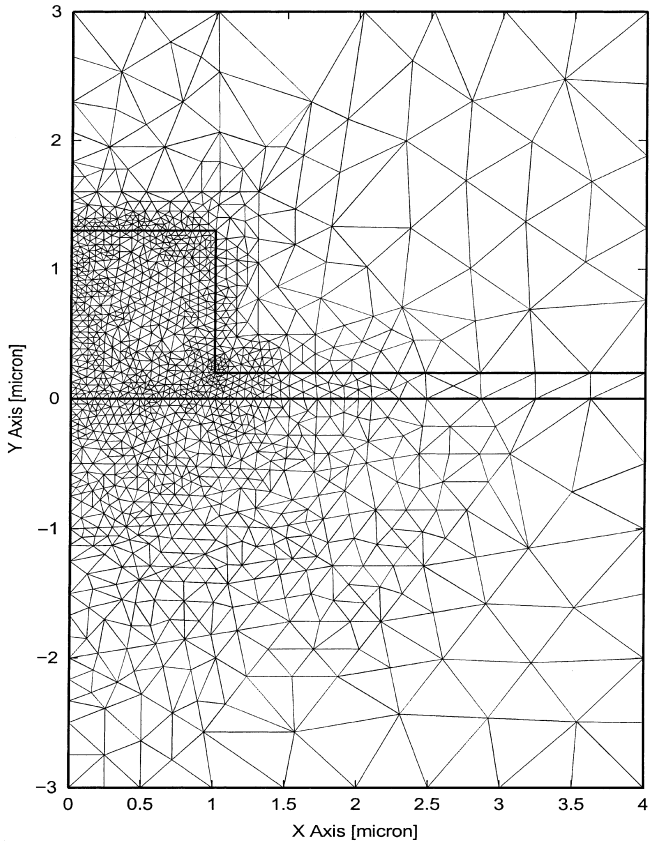

Fig. 2. FEM mesh used for quasi-TE dominant mode of the rib waveguide considered in Table 1. 2556 triangles have been used.

approach. Result for the quasi-TM case is not given in Ramm *et al.* (1997). Note that the lack in available digits in the effective index results shown in Vincetti *et al.* (2000), only four digits are given, allows to check an agreement up to the third digit in B with the results presented here.

Finally, it is important to point out the crucial role of the mesh distribution in order to achieve very accurate FEM solutions. For this reason, all FEM results presented here have been obtained by applying, for each solution looked for, an iterative technique, based on the Delaunay triangulation (Cendes 1983), which, starting from a coarse mesh, increases the number of elements according to a given criterion (Lee 1991; Tsuji and Koshiba 2000). The criterion adopted in this work increases the mesh density in correspondence of steep variations of the amplitude distribution of the three field components. This results in different meshes for each considered mode. As an example the FEM meshes used for quasi-TE and quasi-TM cases are reported in Figs. 2 and 3 and consist, respectively, of 2556 and 2586 triangles.

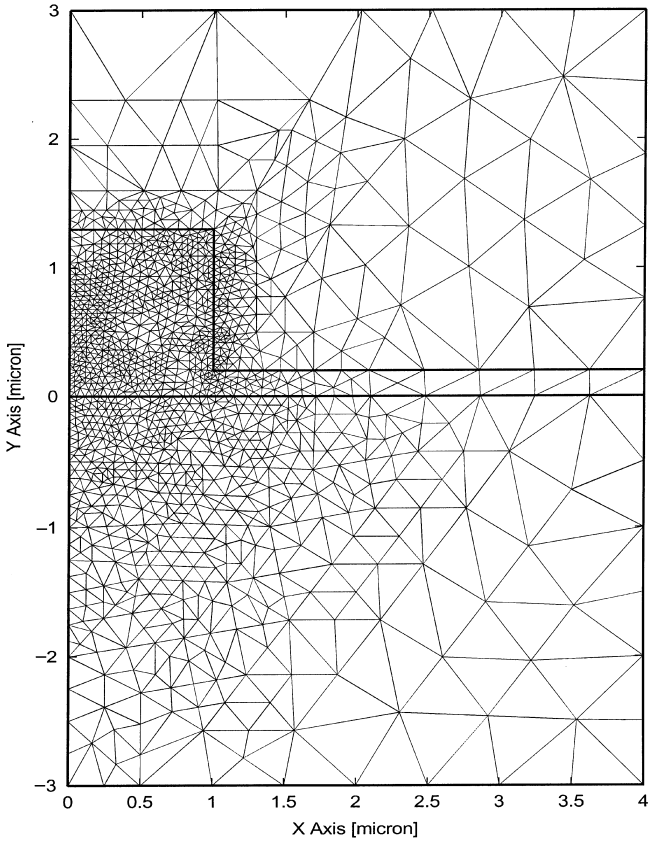

Fig. 3. FEM mesh used for quasi-TM dominant mode of the rib waveguide considered in Table 1. 2586 triangles have been used.

The second example is a classical benchmark test which was used in Vassallo (1997) to compare the accuracy of various methods, as was mentioned in Section 1. The parameters are: $W = 3\,\mu\text{m}$, $H + S = 1.0\,\mu\text{m}$, S within 0.1–$0.9\,\mu\text{m}$, $n_a = 1, n_c = 3.44, n_s = 3.40$ and $\lambda = 1.15\,\mu\text{m}$. For these structures, the enclosing walls were $0.5\,\mu\text{m}$ above the rib and 4–$6\,\mu\text{m}$ below the guiding layer, and the number of TE/TM mode pairs was 100–400 when using MMM; the FEM employed about 2500 triangles in nonuniform meshes for computational regions varying from $4 \times 6\,\mu\text{m}^2$ to $10 \times 7\,\mu\text{m}^2$ according to the considered waveguide. Results for dominant modes are shown in Table 3. Note that the case $S = 0.9$ presented in Vassallo (1997) has not been considered as, in this condition, quasi-TM modes are leaky thus radiating field out of the FEM computational window. Proper open boundary conditions must be introduced to accurately analyze this case and are currently under investigation. The two methods again are in excellent agreement as few unit differences have been obtained on the fifth decimal place, for both

Table 3. B values of dominant modes calculated with MMM and FEM and their difference for the rib waveguide with $W = 3\,\mu m$, $H + S = 1.0\,\mu m$, S within 0.1–0.7 μm, $n_a = 1$, $n_c = 3.44$, $n_s = 3.40$ and $\lambda = 1.15\,\mu m$

S (μm)	MMM	FEM	$\Delta B \times 10^5$
quasi-TE			
0.1	0.30191	0.30188	3
0.3	0.31105	0.31099	6
0.5	0.32702	0.32697	5
0.7	0.35118	0.35117	1
quasi-TM			
0.1	0.26745	0.26745	0
0.3	0.27513	0.27508	5
0.5	0.28899	0.28890	9
0.7	0.31070	0.31063	7

polarizations. These results fully agree with the four-digit reference values given in Vassallo (1997) and, also for the quasi-TM modes which provide differences slightly higher, show an agreement far below the limit of 0.001.

The two approaches have been also applied to the analysis of a lossy structure. In particular the rib waveguide with the following parameters $W = 3\,\mu m, H + S = 1.0\,\mu m, S = 0.5\,\mu m, n_a = 1, \mathrm{Re}(n_c) = 3.44, n_s = 3.40$ and $\lambda = 1.15\,\mu m$ has been analyzed by considering different values of the imaginary part of the core refractive index: 0.001, 0.01 and 0.1. Results are reported in Table 4 showing again high accuracy on both real and imaginary part of the propagation constant.

Finally, the field distributions have been checked. The waveguide parameters were the same as in the second example. Figs. 4 and 5 show profiles of various magnetic field components of dominant quasi-TE and quasi-TM mode, for the case $S = 0.5\,\mu m$. These profiles were generated by MMM, however they are virtually indistinguishable from those generated by FEM on the scale of surface or contour plots presented. In order to compare vector

Table 4. Comparison of the methods for lossy rib waveguide with $W = 3\,\mu m$, $H + S = 1.0\,\mu m$, $S = 0.5\,\mu m$, $n_a = 1$, $\mathrm{Re}(n_c) = 3.44$, $n_s = 3.40$ and $\lambda = 1.15\,\mu m$ for various values of $\mathrm{Im}(n_c)$[a]

Im (n_c)	β_{MMM}	α_{MMM}	β_{FEM}	α_{FEM}	$\delta \times 10^5$
quasi-TE					
0.001	3.413129	0.00079119	3.413126	0.00079115	5
0.01	3.412767	0.0079872	3.412764	0.0079870	3
0.1	3.404330	0.093947	3.404326	0.093948	1
quasi-TM					
0.001	3.411604	0.00075809	3.411599	0.00075812	4
0.01	3.411196	0.0076657	3.411192	0.0076655	3
0.1	3.401469	0.092491	3.401466	0.092491	0

[a] Table shows real (β) and imaginary part (α) of effective mode index of dominant modes calculated with MMM and FEM and relative difference $\delta = |\alpha_{MMM} - \alpha_{FEM}|/\alpha_{MMM}$ of the imaginary part.

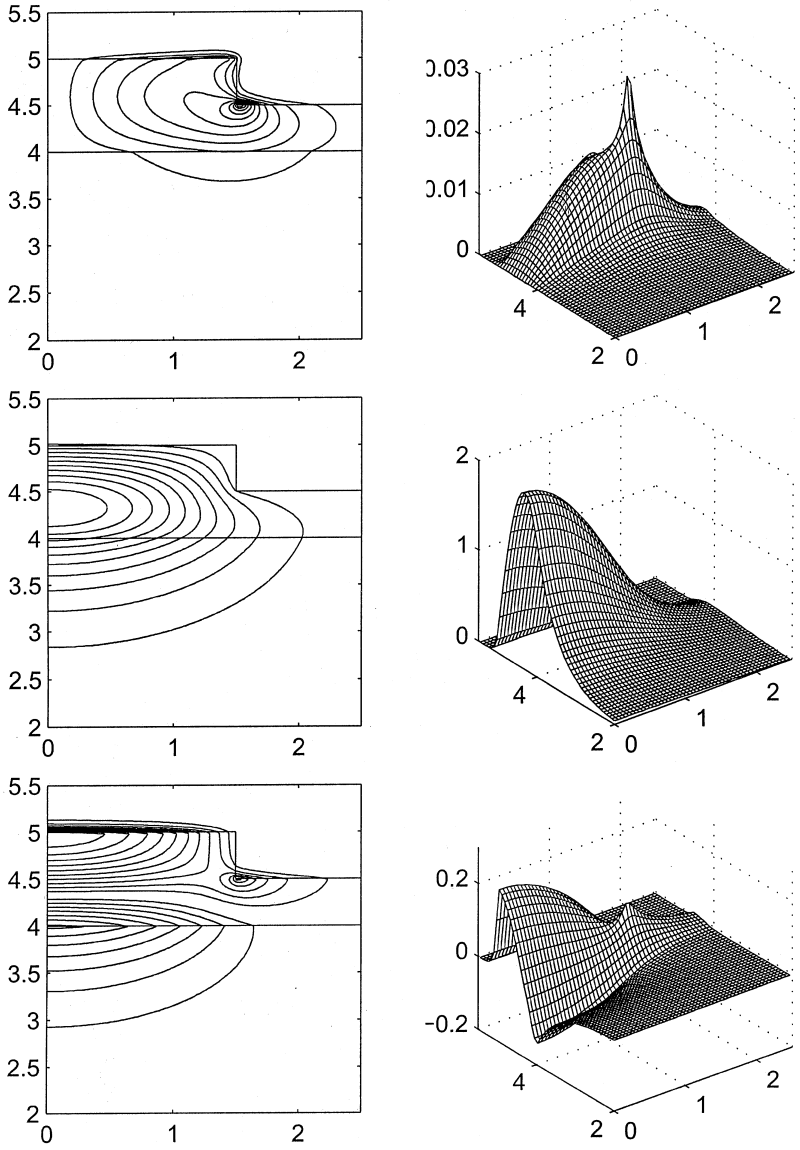

Fig. 4. H_x (top), H_y (center) and H_z (bottom) of quasi-TE dominant mode for the waveguide considered in Table 3 with $S = 0.5\,\mu\text{m}$.

field distributions given by both the methods we calculated the maximum of relative difference

$$\max\left|\frac{F_{\text{MMM}} - F_{\text{FEM}}}{\max|F_{\text{MMM}}|}\right|$$

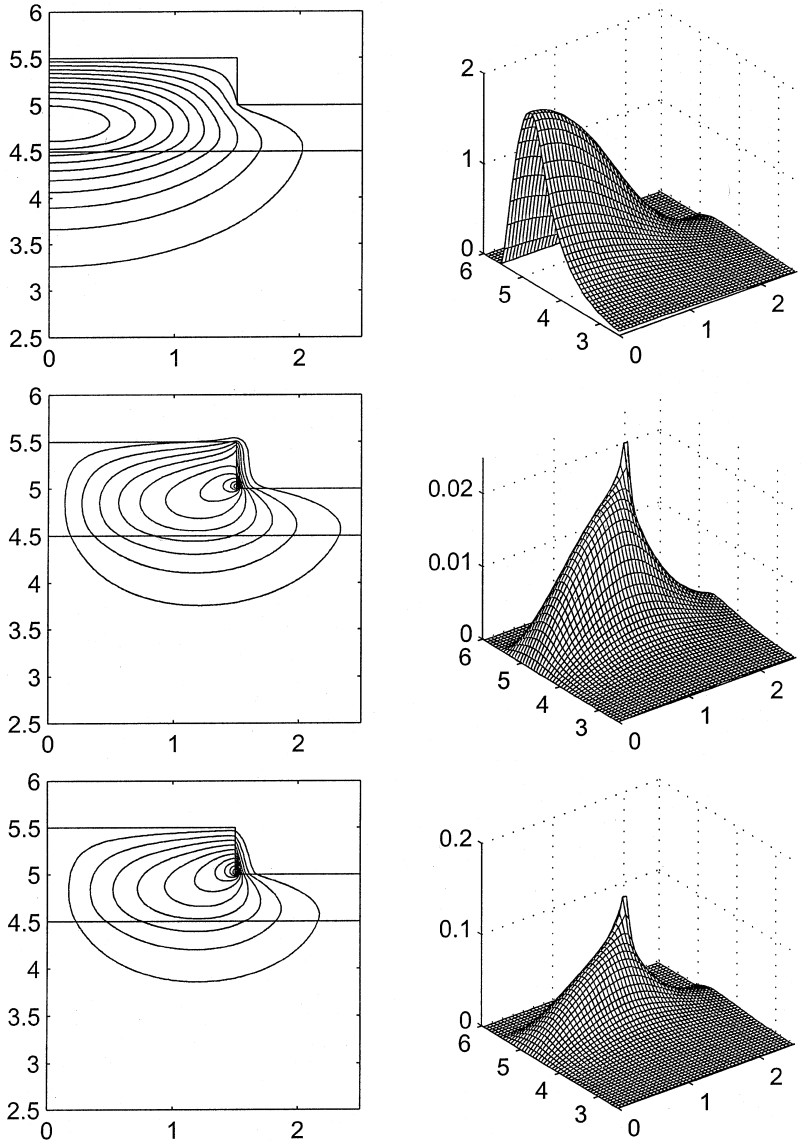

Fig. 5. H_x (top), H_y (center) and H_z (bottom) of quasi-TM dominant mode for the waveguide considered in Table 3 with $S = 0.5\,\mu m$.

where F is any component of H field calculated by MMM or FEM respectively, and max() is maximum of argument in the whole cross-section. The calculated differences in % are shown in Table 5, for both dominant modes and all values of S. Differences in the major components, respectively H_y for quasi-TE and H_x for quasi-TM mode, are less than 1% in all cases. Somewhat worse agreement was obtained for the longitudinal component (H_z) and

Table 5. Maximum of relative difference in % for all components of H-field for the waveguide considered in Table 3[a]

S (μm)	quasi-TE			quasi-TM		
	H_x	H_y	H_z	H_x	H_y	H_z
0.1	11	0.6	4	0.6	23	12
0.3	13	0.9	4	0.6	18	6
0.5	5	0.6	5	0.7	12	7
0.7	8	0.5	8	0.8	7	16

[a] The major components are H_y for quasi-TE mode and H_x for quasi-TM mode, while the other transversal components are the minor ones.

the greatest field differences, about 10–20%, occur in the minor components. This behavior is mainly due to the difference between field values in the waveguide corner and it is the author's belief that these differences can be further reduced. In fact the use of FEM formulations based on Lagrangian nodal basis functions has proved to give better field shapes than those based on edge elements (Selleri *et al.*, this issue).

A few brief remarks on computational efforts and usage of the two methods are necessary. It is author's belief that the increasing performances of computing resources will bring down attention on computational speed which has been for years the main worry of research groups, even to the detriment of other important functionalities. To an extent, high computational times can be accepted if the used approach can assure accuracy, flexibility as well as user friendly, for example graphic, interface and wide applicability.

From this point of view the FEM and the MMM seem to be quite complementary. While the first one can be and has been applied to a huge range of structures with any kind of geometrical shapes, and to a variety of materials, including anisotropic, lossy and nonlinear ones, the MMM can easily tackle only with layered structure and can cope with arbitrary curve or oblique interface only by using staircase approximations. On the contrary, while the FEM require hard effort to be implemented and particular care for the mesh construction, as already observed, the MMM is much more friendly, easily applicable and need less computational resources.

A rigorous speed comparison of the two approaches is a difficult task, being those developed by different research groups which use different computers, with different operating systems and different compilers. Also the mathematical library used to resolve the resulting algebraic system can significantly change time responses. At present, computational times seem to be equivalent and reliable solutions can be obtained in few seconds for both methods using simple PCs. Two examples about the lossless rib waveguide: using a mesh of 2556 triangles the FEM provides full vector solutions in half a minute on a Pentium II PC at 200 MHz using the algebraic solver based on the ARPACK

library (Arpack Software); using 200 TE/TM mode pairs the MMM computational time is the same on PC with AMD Athlon 550 MHz CPU.

4. Conclusions

An accurate comparison of performances provided by FEM and MMM has been presented, considering both real and complex structures. Modal analysis of different kinds of rib waveguides has been performed. Previously published comparisons have been updated showing that the two methods can easily provide solutions in excellent agreement. Although for the kind of structures here analyzed, the exact solutions are not available, the authors think that the good agreement between the two methods, and the considerations about the cited results reported in the literature, allow to identify in B four exact digits after the decimal point. While this conclusion can be questionable and hardly derived when applying a single method, the comparison of two different approaches filters out many factors of uncertainty which cannot be easily controlled due, for example, to the usage of a particular software or hardware resource. For this reason and due to the difficulty in providing reliable error controllers, the authors strongly believe in comparison activity of numerical methods also because, in spite of their wide acceptance for accuracy and efficiency, sometimes they still provide significant differences. This is particularly true for vectorial formulations of mode solvers. Moreover, while acceptable precision can be achieved in B for real structures, still much work must be done for the complex analysis as shown in this paper and in Selleri *et al.* (this issue) as well. Finally the authors strongly invite research groups to deeply investigate the accuracy in the evaluated field often omitted even if crucial for applications where spatial distributions strongly affect the device behavior as, for example, in nonlinear and photonic crystal devices. This is again very important for vectorial formulations which claim to provide all of the components of the unknown field, in particular the minor ones. Deeper analysis of complex solver and field check will be tasks of future researches.

Acknowledgements

The support of this work by Czech MŠMT and the Italian Ministry of Foreign Affairs, in the framework of the Czech–Italian Scientific and Technological Cooperation Program for years 1999 and 2000, and Grant Agency of the Czech Republic (contract 202/98/P274) is gratefully acknowledged. The authors would like to thank anonymous reviewers for their critical suggestions which helped improving the manuscript contents.

References

Arpack Software, available from *http://www.caam.rice.edu/pub/software/ARPACK*.
Bresler, A.D., G.H. Joshi and N. Marcuvitz. *J. Appl. Opt*. **29** 794, 1958.
Cendes, Z.J., D. Shenton and H. Shahnasser. *IEEE Trans. Magn*. **19** 2551, 1983.
Cucinotta, A., S. Selleri, L. Vincetti and M. Zoboli. Open waveguide boundary conditions for finite element modal analysis, *Int. Photon. Res*., Quebec, Canada, 10–15 July, 2000.
Dillon, M.B., P.T.S. Liu and J.P. Webb. *Compel* **13** 311, 1994.
Hernandez-Figueroa, H.E., F.A. Fernandez, Y. Lu and J.B. Davies. *IEEE Trans. Magn*. **31** 1710, 1995.
Koshiba, M., S. Maruyama and K. Hirayama. *J. Lightwave Technol*. **12** 495, 1994.
Koshiba, M. and Y. Tsuji. *J. Lightwave Technol*. **18** 737, 2000.
Lee, J.F. *IEEE Trans. Microwave Theory Tech*. **39** 1262, 1991.
Oliner, A.A., S.T. Peng, T.I. Hsu and A. Sanchez. *IEEE Trans. Microwave Theory Tech*. **29** 855, 1981.
Peng, S.T. and A.A. Oliner. *IEEE Trans. Microwave Theory Tech*. **29** 843, 1981.
Rahman, B.M.A. and J.B. Davies. *IEE Proc. J. Optoelectron*. **132** 349, 1985.
Ramm, K., P.Lüsse and H.-G. Unger. *IEEE Photon. Technol. Lett*. **9** 967, 1997.
Selleri, S. and M. Zoboli. *J. Opt. Soc. Am. A* **14** 1460, 1997.
Selleri, S., L. Vincetti, A. Cucinotta and M. Zoboli. *Opt. Quantum Electron.,* this issue.
Sudbø, A.S. *J. Europ. Opt. Soc*. **2** 211, 1993.
Tsuji, Y. and M. Koshiba. *IEEE J. Selected Topics Quantum Electron*. **6** 163, 2000.
Vassallo, C. *Opt. Quantum Electron*. **29** 95, 1997.
Vincetti, L., A. Cucinotta, S. Selleri and M. Zoboli. *J. Opt. Soc. Amer. A* **17** 1124, 2000.
Yamauchi, J., G. Takahashi and H. Nakano. *J. Lightwave Technol*. **16** 2458, 1998.